

## Microphysics and astrophysics inspired priors for neutron star mergers

SPENCER J. MAGNALL ,<sup>1,2</sup> CHRISTIAN ECKER,<sup>3</sup> LUCIANO REZZOLLA,<sup>3,4,5</sup> AND PAUL D. LASKY <sup>1,2</sup>

<sup>1</sup>*School of Physics and Astronomy, Monash University, Clayton VIC 3800, Australia*

<sup>2</sup>*OzGrav: The ARC Centre of Excellence for Gravitational Wave Discovery, Clayton VIC 3800, Australia*

<sup>3</sup>*Institut für Theoretische Physik, Max-von-Laue-Strasse 1, 60438 Frankfurt, Germany*

<sup>4</sup>*Frankfurt Institute for Advanced Studies, Ruth-Moufang-Strasse 1, 60438 Frankfurt, Germany*

<sup>5</sup>*School of Mathematics, Trinity College, Dublin 2, Ireland*

### ABSTRACT

*Keywords:* neutron stars — gravitational waves — equation of state

### 1. INTRODUCTION

Some background sentences here on the importance and constraints of pQCD and nuclear theory.

When performing gravitational-wave astrophysical inference of binary neutron star mergers (e.g., Abbott et al. 2017, 2018, 2019, 2020), it is common to use ‘agnostic’ priors on their gravitational-wave observables, for example, uniform priors on chirp mass  $\mathcal{M}$  and the dimensionless tidal deformability parameter  $\tilde{\Lambda}$ . However, Altiparmak et al. (2022a) showed that the above conditions imply highly correlated probability distributions in  $\mathcal{M} - \tilde{\Lambda}$  parameter space.

In this work, we advocate using these physics-inspired priors joint priors on  $\mathcal{M}$  and  $\tilde{\Lambda}$ , which are the two best measured and most informative parameters related to the neutron star equation of state. We show an improvement on the measurement of the marginalized posterior on  $\tilde{\Lambda}$  from the gravitational-wave observation of GW170817 from  $\tilde{\Lambda} = \textcolor{red}{XX}$  with the agnostic prior to  $\textcolor{red}{YY}$  with the new physics-inspired prior. This corresponds to an improvement in the neutron star radius measurement of an equivalent  $[1.4] M_{\odot}$  star from  $\textcolor{red}{R}_{1.4} = \text{to } \dots$ . For GW190425, the improvement is  $\dots$ .

We also demonstrate the utility of these priors for distinguishing between the sources of Gravitational wave events. We perform model selection between a binary neutron star and neutron star – black hole origin of GW190425 and find a Bayes factor of  $\textcolor{red}{XX}$  in favor of a binary neutron star origin.

In advocating for this prior becoming standard in the literature, we provide an open-source configuration for the BILBY Bayesian inference library (Ashton et al. 2019; Romero-Shaw et al. 2020) currently used for the majority of gravitational-wave parameter estimation by the LIGO-Virgo-KAGRA collaboration (Asasi et al.

2015; Acernese et al. 2015; Akutsu et al. 2020). This implements numerically the joint probability distribution as a constrained prior for  $\mathcal{M}$  and  $\tilde{\Lambda}$  as described in the next section.

### 2. METHODS

Methodology for the speed of sound parameterisation, and eos generation and constraints should go here.

Our setup closely follows that of Altiparmak et al. (2022b), which we briefly review here. We begin by constructing a large set of EOSs by stitching together various components. At the lowest densities ( $n < 0.5n_s$ ), we adopt the Baym-Pethick-Sutherland (BPS) model (Baym et al. 1971) for the neutron-star crust. In the range  $0.5n_s < n < 1.1n_s$ , we randomly sample polytropes to span the range between the softest and stiffest EOSs from Hebeler et al. (2013). At high densities ( $n \gtrsim 40, n_s$ ), corresponding to a baryon chemical potential of  $\mu = 2.6, \text{GeV}$ , we impose the perturbative QCD constraint from ? on the pressure  $p(X, \mu)$  of cold quark matter, with the renormalization scale parameter  $X$  sampled uniformly in  $[1, 4]$ .

For the intermediate density range ( $1.1n_s < n \lesssim 40n_s$ ), we use the parametrization method of Annala et al. (2020), which models the sound speed as a function of the chemical potential,  $c_s^2(\mu)$ , using piecewise-linear segments:

$$c_s^2(\mu) = \frac{(\mu_{i+1} - \mu) c_{s,i}^2 + (\mu - \mu_i) c_{s,i+1}^2}{\mu_{i+1} - \mu_i}, \quad (1)$$

where  $\mu_i$  and  $c_{s,i}^2$  are parameters defining the  $i$ -th segment in the range  $\mu_i \leq \mu \leq \mu_{i+1}$ . Throughout this work, we adopt natural units where  $c = G = 1$ .

The number density follows as

$$n(\mu) = n_1 \exp \left( \int_{\mu_1}^{\mu} \frac{d\mu'}{\mu' c_s^2(\mu')} \right), \quad (2)$$

where  $n_1 = 1.1$ ,  $n_s$ , and  $\mu_1 = \mu(n_1)$  is set by the corresponding polytropic EOS. The pressure is then obtained via

$$p(\mu) = p_1 + \int_{\mu_1}^{\mu} d\mu' n(\mu') , \quad (3)$$

where the integration constant  $p_1$  matches the pressure of the polytrope at  $n = n_1$ . We numerically integrate Eq. (3) using seven segments for  $c_s^2(\mu)$ .

Using this framework, we generate  $XXX$  EOSs by randomly selecting the maximum sound speed  $c_{s,\max}^2 \in [0, 1]$  and uniformly sampling the free parameters  $\mu_i \in [\mu_1, \mu_{N+1}]$  (where  $\mu_{N+1} = 2.6\text{GeV}$ ) and  $c_{s,i}^2 \in [0, c_{s,\max}^2]$ . These EOSs are consistent with nuclear theory and perturbative QCD uncertainties.

To incorporate astrophysical constraints, we solve the Tolman-Oppenheimer-Volkoff (TOV) equations for each EOS and retain only those satisfying the mass measurements of J0348+0432 (Antoniadis et al. 2013) ( $M = 2.01 \pm 0.04, M_\odot$ ) and J0740+6620 (Cromartie et al. 2020; Fonseca et al. 2021) ( $M = 2.08 \pm 0.07, M_\odot$ ), discarding EOSs with a maximum mass  $M_{\text{TOV}} < 2.0, M_\odot$ . We also impose NICER radius constraints from J0740+6620 (Miller et al. 2021; Riley et al. 2021) and J0030+0451 (Riley et al. 2019; Miller et al. 2019), rejecting EOSs with  $R < 10.75$  km at  $M = 2.0, M_\odot$  or  $R < 10.8$  km at  $M = 1.1, M_\odot$ .

In the neutron star binary case, the binary tidal deformability is computed as

$$\tilde{\Lambda}_{\text{NSNS}} = \frac{16}{13} \frac{(12M_2 + M_1)M_1^4\Lambda_1 + (12M_1 + M_2)M_2^4\Lambda_2}{(M_1 + M_2)^5} , \quad (4)$$

where  $M_i$ ,  $R_i$ , and  $\Lambda_i = \frac{2}{3}k_2(R_i/M_i)^5$  ( $i = 1, 2$ ) denote the component masses, radii, and tidal deformabilities, with  $k_2$  being the second tidal Love number. The chirp mass is given by  $\mathcal{M}_{\text{chirp}} = (M_1M_2)^{3/5}(M_1 + M_2)^{-1/5}$  and we in the following we will use the mass ratio defined as  $q = M_2/M_1$ .

In the mixed binary case, i.e., where one binary component is a neutron star and the other one a black hole, the formula for the binary tidal deformability simplifies, because black holes have zero tidal deformability  $\Lambda_{\text{BH}} = 0$ . The binary tidal deformability in this case becomes

$$\tilde{\Lambda}_{\text{NSBH}} = \frac{16}{13} \frac{(12M_{\text{BH}} + M_{\text{NS}})M_{\text{NS}}^4\Lambda_{\text{NS}}}{(M_{\text{NS}} + M_{\text{BH}})^5} , \quad (5)$$

where  $M_{\text{NS}}$  and  $\Lambda_{\text{NS}}$  are the neutron star mass and tidal deformability, respectively, and  $M_{\text{BH}}$  the black hole mass. The expressions for the chirp mass and mass ratio remain intact, with the understanding that  $M_1 = M_{\text{NS}}$  and  $M_2 = M_{\text{BH}}$ .

## 2.1. Binary neutron star mergers

We use the probability distribution of  $10^7$  equation of state models informed by nuclear physics, perturbative quantum chromodynamics and astrophysics from Altiparmak et al. (2022a) to generate a probability distribution for chirp mass – tidal deformability, and use it as priors on those quantities as shown in Fig. 1. We implement this in BILBY using the `conditional_prior` function<sup>1</sup>, interpolating the  $200 \times 200$  grid to draw from a joint prior on  $\mathcal{M}$  and  $\tilde{\Lambda}$ .

We sample directly in source-frame chirp mass, mass ratio  $q = m_1/m_2$  and the two tidal deformability parameters  $\tilde{\Lambda}$  and  $\delta\tilde{\Lambda}$  (see Favata 2014; Wade et al. 2014, for explicit expressions for these quantities). We note that  $q$  is not a variable that depends on the equation of state, but instead priors *could* be chosen based on astrophysical formation scenarios. In this work, we take the standard approach and choose a prior on  $q$  that is uniform between  $q = 0.125$  and  $1$  (e.g., Romero-Shaw et al. 2020).

We further note that, while both  $\tilde{\Lambda}$  and  $\delta\tilde{\Lambda}$  are related to the equation of state, we only impose a prior here on  $\tilde{\Lambda}$ . In general,  $\tilde{\Lambda}$  is measured much better than  $\delta\tilde{\Lambda}$ , which can be understood because  $\tilde{\Lambda}$  enters waveform approximates at the 5<sup>th</sup> post-Newtonian order, whereas  $\delta\tilde{\Lambda}$  only enters at 6<sup>th</sup> in linear combination with  $\tilde{\Lambda}$  (Wade et al. 2014). In principle, one could set a combined prior on the three parameters  $(\mathcal{M}, \tilde{\Lambda}, \delta\tilde{\Lambda})$ , however, adding this latter parameter would not add significantly to parameter estimation in the relatively low signal-to-noise regime because of the above arguments.

## 2.2. Neutron star – black hole mergers

The parameterisation in the previous section does not go to high enough values of chirp mass because it is assumed both stars in the merger are neutron star. We therefore derive a new distribution for neutron star–black hole mergers by going back to the raw distributions of progenitor stellar masses and radii, and combining that progenitor with a black hole of mass  $m_1$  and tidal deformability  $\Lambda_1 = 0$ . We use a uniform distributed mass ratio to generate our prior relationship. We have found more sophisticated mass-ratio distributions, such as those informed by state of the art binary population synthesis (e.g Broekgaarden et al. 2021) did not significantly impact the shape of the prior distribution. We demonstrate the independence of our results on the chosen population model in Appendix A. We choose once again to work with priors in  $\mathcal{M} - \tilde{\Lambda}$ , en-

<sup>1</sup> git link to our code!?

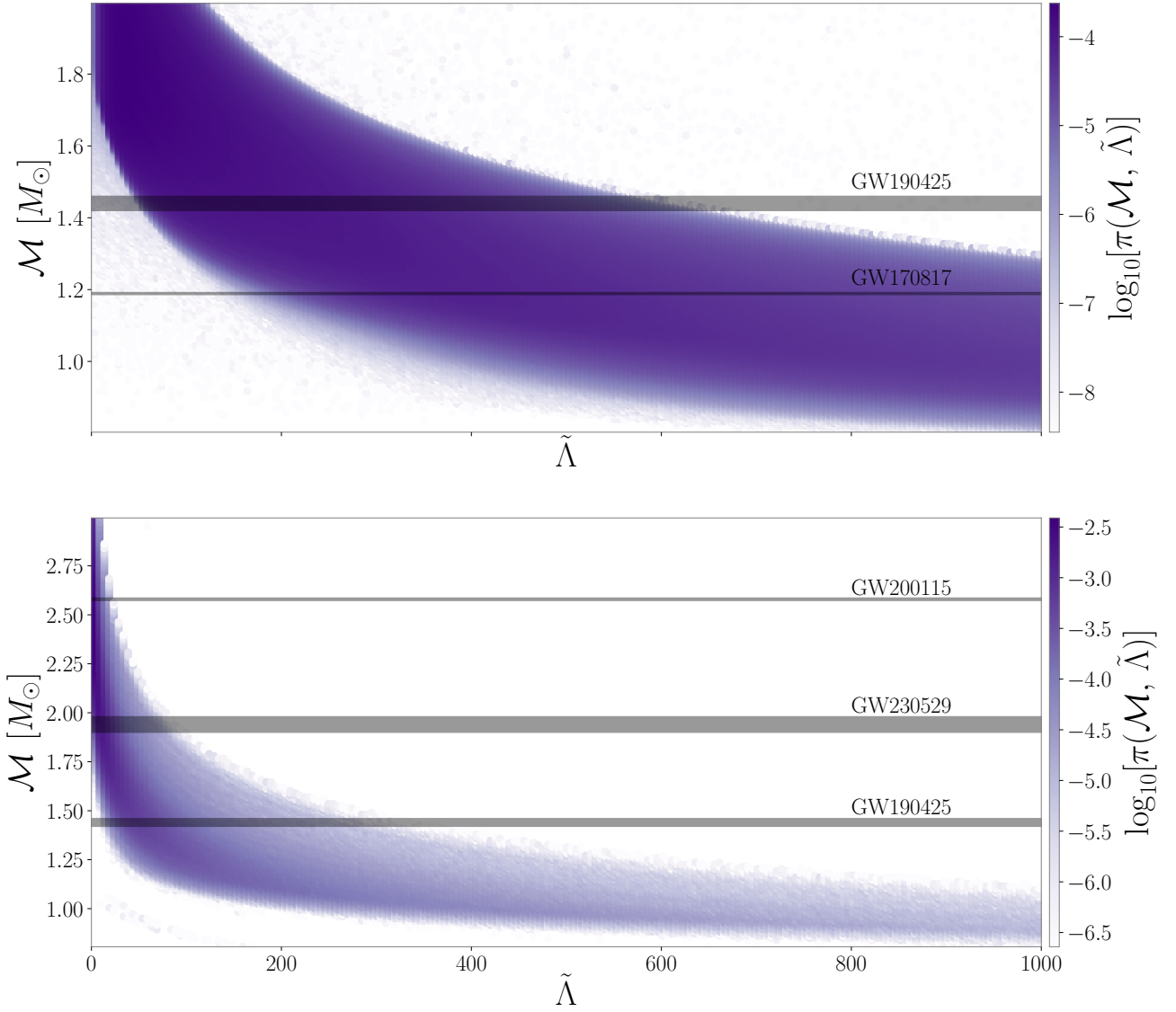


**Figure 1.** Coupled priors for the source-frame chirp mass  $\mathcal{M}$  and dimensionless tidal deformability  $\tilde{\Lambda}$ . Top: prior for binary neutron star mergers. Bottom: prior for neutron star – black hole mergers. The horizontal grey bands are the 90% credible intervals for the measured chirp masses of GW170817 (Abbott et al. 2017), GW190425 (Abbott et al. 2020), GW200115 (Abbott et al. 2021) and GW230529 (Abac et al. 2024)

forcing  $\tilde{\Lambda}(\Lambda_2, \mathcal{M}, q)$  where  $\Lambda_2$  is the tidal deformability of the lighter object in the binary, which we assume is the neutron star.

### 2.3. Parameter estimation

We perform Bayesian parameter estimation on the Gravitational-Wave strain data of the two (likely) binary neutron star merger events GW170817 and GW190425 using the strain data freely available from the GWOSC repository<sup>2</sup>. We utilize the BILBY Bayesian inference framework and priors on source-frame chirp mass and tidal-deformability implemented in Section 2. Priors for all renaming parameters assume the low-spin ( $\chi \leq 0.05$ ) defaults as defined in BILBY (e.g Ashton et al. 2019, Romero-Shaw et al. 2020).

Parameter estimation for each run was performed using the DYNESTY nested sampler (Speagle 2020) and the IMRPhenomPv2\_NRTIDAL waveform (Dietrich et al. 2019). Analysis of binary neutron star merger signals is significantly computationally expensive and as such we utilize PBILBY (Smith et al. 2020), a parallel implementation of BILBY which uses the Message Passing Interface (MPI).

Since we are required to sample in the source-frame chirp mass instead of the observer frame, we must assume a cosmology. We use  $H_0 = 67.66 \text{ km s}^{-1}$ ,  $\Omega_M = 0.30966$  informed by the Planck 2018 results (Planck Collaboration et al. 2020).

We employ both the binary neutron star and the neutron star – black hole merger priors in our analysis of GW190425. This facilitates a model selection analysis between a binary neutron star, and neutron star – black hole origin of GW190425. The details of this model selection analysis are described further in Appendix B. For GW170817 we perform parameter estimation using the binary neutron star prior only.

We reconstruct mass–radius curves from posterior samples of source-frame chirp and tidal deformability using ...

## 3. RESULTS

### 3.1. GW170817

Figure 2 shows the posterior distributions of intrinsic tidal parameter of GW170817 analyzed using the  $\mathcal{M}-\tilde{\Lambda}$  feature (teal), when compared to the official posterior samples from the LVK (midnight blue). While we show only the tidal posteriors, we sample over all binary parameters. The full posteriors for this event are shown in Appendix XX.

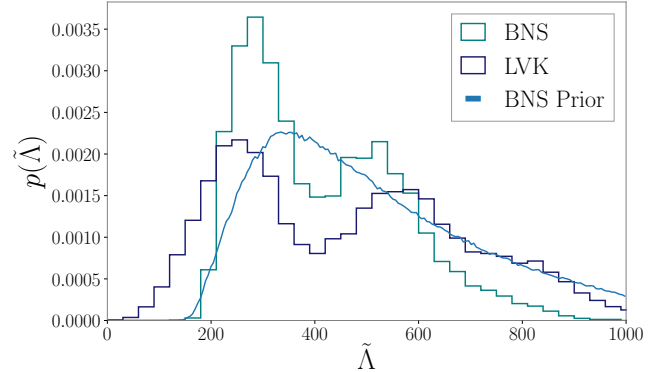


**Figure 2.** The posterior distributions of the tidal deformability  $\tilde{\Lambda}$  obtained from Bayesian parameter estimation for GW170817. The posterior using a nuclear, microphysics, and astrophysics inspired prior is shown in teal, while the posterior using uniform priors from the LVK is shown in midnight blue. We show the (marginalized) prior with the light blue curve. Note, the posterior samples from the LVK show support up to  $\tilde{\Lambda} = 2000$ .

Figure XX shows the reconstructed mass–radius curves of GW170817 ...

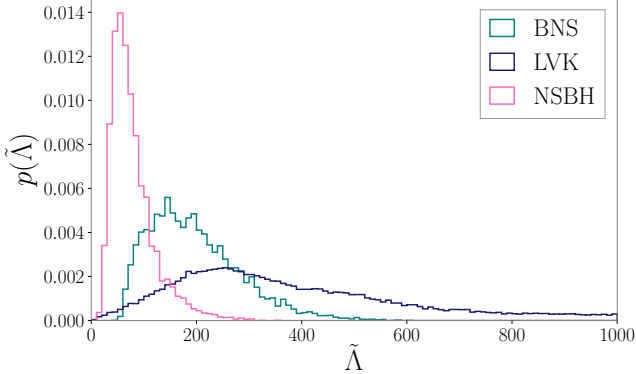
### 3.2. GW190425

Figure 3 shows the posterior distribution of the intrinsic tidal parameter of GW190425 when analyzed using both the binary neutron star prior (teal) and neutron star – black hole prior (pink). We show the official posterior distribution of the LVK obtained using uniform priors in blue. Bayesian model selection between the binary neutron star and neutron star – black hole merger gives a Bayes factor of XX, slightly in favor of a binary neutron star merger origin. Figure XX shows the reconstructed mass radius curves of GW190425 analyzed using the new priors.

## 4. CONCLUSIONS

## APPENDIX

<sup>2</sup> <https://gwosc.org>



**Figure 3.** The posterior distributions of the tidal deformability  $\tilde{\Lambda}$  obtained from Bayesian parameter estimation for G190425. The posterior using a nuclear, microphysics, and astrophysics inspired binary neutron star prior is shown in teal, and the corresponding neutron star – black hole prior is shown in pink. The posterior using uniform priors from the LVK is shown in midnight blue.

### A. NEUTRON STAR – BLACK HOLE MERGER PRIOR GENERATION

We should detail the prior generation for neutron star – black hole here, in particular the independence of a mass ratio informed by population synthesis on the prior distributions and potentially the resultant posterior distributions. Might be worth showing an extreme example to prove the point.

We generate two relations, one with uniform priors on our population of BH - NS mergers, and one directly informed by state of the art binary population synthesis. We use the mass ratio distribution of Broekgaarden et al. (2021) ([what particular model are we using?](#)) for the generation of our population synthesis informed priors. Figure 4 shows the distribution in mass ratio used for the generation of the prior.

### B. MODEL SELECTION

### REFERENCES

- Aasi, J., Abbott, B. P., Abbott, R., et al. 2015, Classical and Quantum Gravity, 32, 074001, doi: [10.1088/0264-9381/32/7/074001](https://doi.org/10.1088/0264-9381/32/7/074001)
- Abac, A. G., Abbott, R., Abouelfettouh, I., et al. 2024, ApJL, 970, L34, doi: [10.3847/2041-8213/ad5beb](https://doi.org/10.3847/2041-8213/ad5beb)
- Abbott, B. P., Abbott, R., Abbott, T. D., et al. 2017, PhRvL, 119, 161101, doi: [10.1103/PhysRevLett.119.161101](https://doi.org/10.1103/PhysRevLett.119.161101)
- . 2018, PhRvL, 121, 161101, doi: [10.1103/PhysRevLett.121.161101](https://doi.org/10.1103/PhysRevLett.121.161101)
- . 2019, Physical Review X, 9, 011001, doi: [10.1103/PhysRevX.9.011001](https://doi.org/10.1103/PhysRevX.9.011001)
- . 2020, ApJL, 892, L3, doi: [10.3847/2041-8213/ab75f5](https://doi.org/10.3847/2041-8213/ab75f5)
- Abbott, R., Abbott, T. D., Abraham, S., et al. 2021, ApJL, 915, L5, doi: [10.3847/2041-8213/ac082e](https://doi.org/10.3847/2041-8213/ac082e)
- Acernese, F., Agathos, M., Agatsuma, K., et al. 2015, Classical and Quantum Gravity, 32, 024001, doi: [10.1088/0264-9381/32/2/024001](https://doi.org/10.1088/0264-9381/32/2/024001)
- Akutsu, T., Ando, M., Arai, K., et al. 2020, Progress of Theoretical and Experimental Physics, 2021, 05A101, doi: [10.1093/ptep/ptaa125](https://doi.org/10.1093/ptep/ptaa125)
- Altiparmak, S., Ecker, C., & Rezzolla, L. 2022a, ApJL, 939, L34, doi: [10.3847/2041-8213/ac9b2a](https://doi.org/10.3847/2041-8213/ac9b2a)
- . 2022b, Astrophys. J. Lett., 939, L34, doi: [10.3847/2041-8213/ac9b2a](https://doi.org/10.3847/2041-8213/ac9b2a)
- Annala, E., Gorda, T., Kurkela, A., Näättilä, J., & Vuorinen, A. 2020, Nature Physics, 16, 907, doi: [10.1038/s41567-020-0914-9](https://doi.org/10.1038/s41567-020-0914-9)
- Antoniadis, J., Freire, P. C. C., Wex, N., et al. 2013, Science, 340, 448, doi: [10.1126/science.1233232](https://doi.org/10.1126/science.1233232)
- Ashton, G., Hübner, M., Lasky, P. D., et al. 2019, ApJS, 241, 27, doi: [10.3847/1538-4365/ab06fc](https://doi.org/10.3847/1538-4365/ab06fc)
- Baym, G., Pethick, C., & Sutherland, P. 1971, ApJ, 170, 299, doi: [10.1086/151216](https://doi.org/10.1086/151216)
- Broekgaarden, F. S., Berger, E., Neijssel, C. J., et al. 2021, MNRAS, 508, 5028, doi: [10.1093/mnras/stab2716](https://doi.org/10.1093/mnras/stab2716)

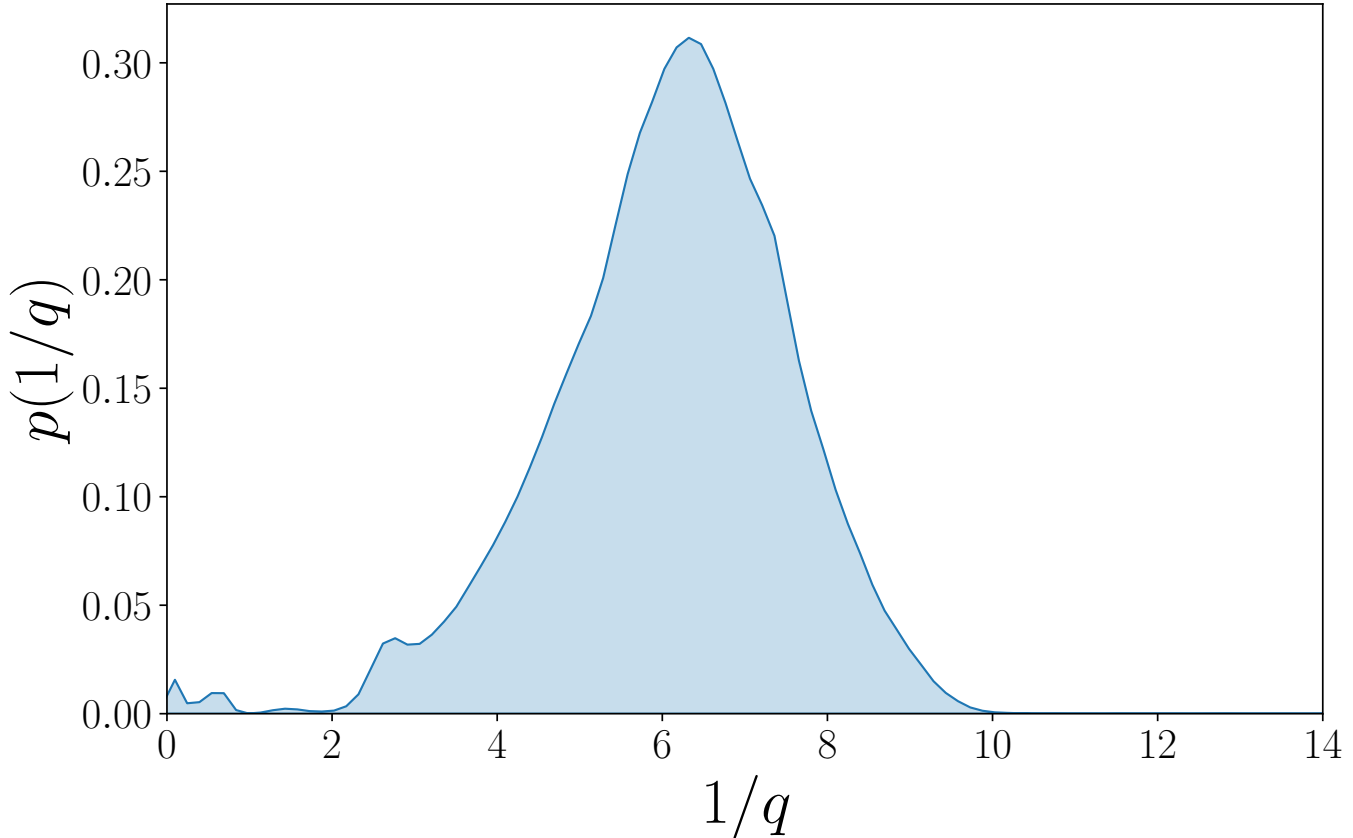


**Figure 4.** Probability density function of the mass ratio for detectable neutron star black hole mergers from (Broekgaarden et al. 2021).

Cromartie, H. T., Fonseca, E., Ransom, S. M., et al. 2020,  
Nature Astronomy, 4, 72, doi: [10.1038/s41550-019-0880-2](https://doi.org/10.1038/s41550-019-0880-2)

Dietrich, T., Samajdar, A., Khan, S., et al. 2019, PhRvD,  
100, 044003, doi: [10.1103/PhysRevD.100.044003](https://doi.org/10.1103/PhysRevD.100.044003)

Favata, M. 2014, PhRvL, 112, 101101,  
doi: [10.1103/PhysRevLett.112.101101](https://doi.org/10.1103/PhysRevLett.112.101101)

Fonseca, E., Cromartie, H. T., Pennucci, T. T., et al. 2021,  
Astrophys. J. Lett., 915, L12,  
doi: [10.3847/2041-8213/ac03b8](https://doi.org/10.3847/2041-8213/ac03b8)

Hebeler, K., Lattimer, J. M., Pethick, C. J., & Schwenk, A.  
2013, Astrophys. J., 773, 11,  
doi: [10.1088/0004-637X/773/1/11](https://doi.org/10.1088/0004-637X/773/1/11)

Miller, M. C., Lamb, F. K., Dittmann, A. J., et al. 2019,  
Astrophys. J. Lett., 887, L24,  
doi: [10.3847/2041-8213/ab50c5](https://doi.org/10.3847/2041-8213/ab50c5)

—. 2021, Astrophys. J. Lett., 918, L28,  
doi: [10.3847/2041-8213/ac089b](https://doi.org/10.3847/2041-8213/ac089b)

Planck Collaboration, et al. 2020, A&A, 641, A6,  
doi: [10.1051/0004-6361/201833910](https://doi.org/10.1051/0004-6361/201833910)

Riley, T. E., Watts, A. L., Bogdanov, S., et al. 2019,  
Astrophys. J. Lett., 887, L21,  
doi: [10.3847/2041-8213/ab481c](https://doi.org/10.3847/2041-8213/ab481c)

Riley, T. E., Watts, A. L., Ray, P. S., et al. 2021,  
Astrophys. J. Lett., 918, L27,  
doi: [10.3847/2041-8213/ac0a81](https://doi.org/10.3847/2041-8213/ac0a81)

Romero-Shaw, I. M., Talbot, C., Biscoveanu, S., et al. 2020,  
MNRAS, 499, 3295, doi: [10.1093/mnras/staa2850](https://doi.org/10.1093/mnras/staa2850)

Smith, R. J. E., Ashton, G., Vajpeyi, A., & Talbot, C.  
2020, MNRAS, 498, 4492, doi: [10.1093/mnras/staa2483](https://doi.org/10.1093/mnras/staa2483)

Speagle, J. S. 2020, MNRAS, 493, 3132,  
doi: [10.1093/mnras/staa278](https://doi.org/10.1093/mnras/staa278)

Wade, L., Creighton, J. D. E., Ochsner, E., et al. 2014,  
PhRvD, 89, 103012, doi: [10.1103/PhysRevD.89.103012](https://doi.org/10.1103/PhysRevD.89.103012)